Theory of Light Quenching: Effects on Fluorescence Polarization, Intensity, and Anisotropy Decays

Józef Kuśba, Valery Bogdanov, Ignacy Gryczynski, and Joseph R. Lakowicz
Center for Fluorescence Spectroscopy, Department of Biological Chemistry, University of Maryland at Baltimore, School of Medicine, Baltimore, Maryland 21201, USA

ABSTRACT Experimental studies have recently demonstrated that fluorescence emission can be quenched by laser light pulses from modern high repetition rate lasers, a phenomenon we call "light quenching." We now describe the theory of light quenching and some of its effects on the steady-state and time-resolved intensity and anisotropy decays of fluorophores. Light quenching can decrease or increase the steady-state or time-zero anisotropy. Remarkably, the light quenching can break the usual z axis symmetry of the excited-state population, and the emission polarization can range from -1 to $+1$ under selected conditions. The measured anisotropy (or polarization) depends upon whether the observation axis is parallel or perpendicular to the propagation direction of the light quenching beam. The effects of light quenching are different for a single pulse, which results in both excitation and quenching, as compared with a time-delayed quenching pulse. Time-delayed light quenching pulses can result in step-like changes in the time-dependent intensity or anisotropy and are predicted to cause oscillations in the frequency-domain intensity and anisotropy decays. The increasing availability of pulsed laser sources offers the opportunity for a new class of two-pulse or multiple-pulse experiments where the sample is prepared by an excitation pulse, the excited state population is modified by the quenching pulse(s), followed by time- or frequency-domain measurements of the resulting emission.

INTRODUCTION

Time-resolved fluorescence is widely used to study the structure and dynamics of biological macromolecules and assemblies (Dewey, 1991; Jameson and Reinhart, 1989; Lakowicz, 1992; Demehenko, 1986). Such experiments can be performed by time-domain (TD) (O'Connor and Phillips, 1984; Demas, 1983; Fleming, 1986) or frequency-domain (FD) (Lakowicz and Gryczynski, 1991; Baeyens et al., 1991; Klein, 1984) methods. To date, all such studies used one light pulse or a single amplitude-modulated beam for excitation (preparation) of the sample, followed by measurement of the intensity or anisotropy decay of the emission. In recent years, there has been an increased use of the intense light pulses from picosecond (ps) or femtosecond (fs) dye lasers, which allow two-photon excitation (TPE) of biochemical fluorophores (Lakowicz et al., 1992a–c; Lakowicz and Gryczynski, 1992; Szmacinski et al., 1993) and can provide localized "confocal" excitation in fluorescence microscopy (Denk et al., 1990; Piston et al., 1992). The use of intense pulses can result in other effects, such as depletion of the ground state population (Ansari and Szabo, 1993) or local photobleaching of the sample (Koppel et al., 1986).

We now describe the theory for a heretofore unconsidered effect of using intense laser pulses: quenching of the excited state population by stimulated emission. If the wavelength of the quenching pulse overlaps the emission spectrum of the fluorophore, then the fluorophore can be stimulated to emit, as predicted by Einstein (1917). Because the emitted photon is directed along the path of the quenching beam, this photon cannot be observed with right-angle or small-angle observation conditions, resulting in a decrease (quenching) of the observed intensity.

In a recent publication, we demonstrated that light quenching could be observed using modern high repetition rate lasers (Lakowicz et al., 1994), whereas earlier observation of light quenching used giant pulses from Ruby lasers. In the present report, we describe the effects of light quenching on the steady-state emission anisotropy or polarization, in the absence of rotation diffusion, and how these values depend on the polarization of the laser beam and the axis of observation. Depending on the polarization of the excitation and quenching beams, light quenching can increase or decrease the anisotropy. The extents of light quenching and changes in anisotropy are different for continuous or pulsed illumination, and depend on the polarization orientation of the quenching beam and the angle of observation. Surprisingly, the changes in polarization are different for a quenching pulse that is co-incident or time-delayed relative to the excitation pulse. Under appropriate conditions, light quenching can break the usual z axis cylindrical symmetry and result in polarization values as high as unity.

We also describe a phenomenological theory of the effects of light quenching on the intensity and anisotropy decays with rotation diffusion, as observed by 'time-domain or

Received for publication 10 May 1994 and in final form 19 August 1994.

Address reprint requests to Dr. Joseph R. Lakowicz, Department of Biological Chemistry, University of Maryland School of Medicine, 108 N. Greene St., Baltimore, MD 21201-1503. Tel.: 410-706-7978; Fax: 410-706-8408; E-mail: jf@sg.ab.umd.edu.

Dr. Kuśba is on leave from Technical University of Gdańsk, Faculty of Applied Physics and Mathematics, ul. Narutowicza 11/12, 80-952 Gdańsk, Poland.

Abbreviations used: ADTM, angular distribution of transition moments of the excited molecules; FD, frequency-domain; LQ, light quenching; OPE, one-photon excitation; TD, time-domain; TPE, two-photon excitation.

0006-3495/94/11/2024/17 $2.00

frequency-domain methods. The effects of non-co-linear transition moments, multiple lifetimes, multiple correlation times, spectral relaxation, pulse width, and other phenomena on light quenching are presently being investigated and will be reported elsewhere. The effects of light quenching are complex, often counter-intuitive, and a complete understanding will require additional theoretical and experimental studies. Nonetheless, this phenomenon appears to be rich with information, and light quenching may offer new opportunities for the design of steady-state and time-resolved fluorescence experiments.

THEORY AND RESULTS

One can imagine two classes of light quenching experiments. The simplest experimental situation is when the excitation and quenching is provided by the same light pulse (Fig. 1, *left*), in which case the pulses are coincident in time and direction of propagation. The second class of light quenching experiments constitute situations when the excitation and quenching are provided by different light pulses. In the latter case, the excitation and quenching beam may be not coincident in time, direction of propagation, or polarization. These two classes of light quenching experiments will be referred to as one-pulse (one-beam) or two-pulse (two-beam) light quenching, respectively. In the two-pulse experiments, the polarization of the quenching pulse may be arbitrarily oriented relatively to the polarization direction of the exciting pulse. We restrict ourselves to the cases where these polarizations are either parallel (parallel two-pulse quenching, Fig. 1, *middle*) or perpendicular (perpendicular two-pulse quenching, Fig. 1, *right*). We note that the use of light pulses does not imply time-resolved measurements. For the initial discussion, we consider steady-state measurements while the sample is illuminated with a continuous series of excitation and quenching pulses.

A general description of light quenching requires consideration of the spectral and dynamic properties of the fluorophores, orientation of the transition moments, and laser pulse width(s), which is beyond the scope of a single report. In the present report, we assume that the widths of the excitation and quenching pulses are small compared with the excited-state lifetime. We also assume that the absorption and emission moments are colinear (Fig. 2) and that rotational diffusion does not occur during the excited-state lifetime. This latter restriction is removed for discussion of the time-dependent intensity and anisotropy decays, using a phenomenological model. And finally, we assume that the ground state population is not significantly altered by the excitation pulse. Such effects can be avoided if the absorption of the sample is small, as is possible with long wavelength one-photon (OPE) or two-photon excitation (TPE).

To introduce the concept of light quenching, we briefly describe the expected results for one-pulse (one-beam) and two-pulse (two-beam) light quenching. A central concept is that light quenching displays the same photoselection properties as does light absorption (Michl and Thulstrup, 1986). That is, the probabilities of absorption and light quenching are both proportional to $\cos^2\theta$, where θ is the angle between the electric vector of the incident light and the transition moment for absorption or emission, respectively. Consequently, light quenching can selectively deplete just part of the excited-state population with the appropriate orientation. In contrast, collisional quenching depletes all orientations with equal probability. Also, in contrast to collisional quenching, light quenching can act only during a small fraction of the intensity decay and is easily reversible by blocking the quenching beam.

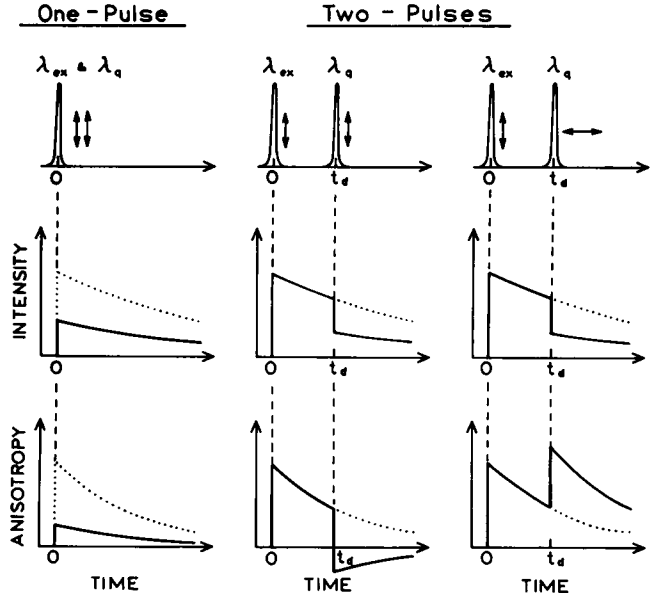

FIGURE 1 Intuitive description of the effects of light quenching on the intensity and anisotropy decays of fluorescence for one-pulse (*left*) and two-pulse (*center* and *right*) experiments. The effects caused by light quenching are shown by the solid lines. The dotted lines show the shape of the intensity and/or anisotropy decays in the absence of light quenching.

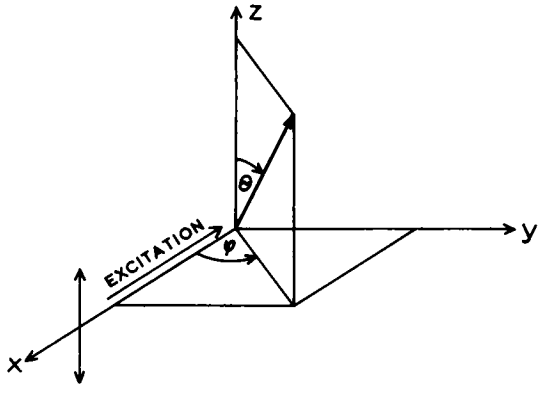

FIGURE 2 Coordinate system for the light quenching. The x axis is parallel to the propagation direction of the excitation. The fluorophore's absorption and emission transition moments are assumed colinear. The angles of the transition moment from the z and x axis are given by θ and φ, respectively.

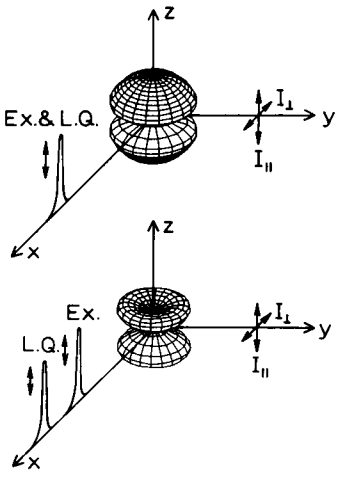

FIGURE 3 Light quenching with cylindrical symmetry around the z axis. The top scheme shows one-pulse light quenching, and the bottom scheme shows parallel two-pulse light quenching. The polar plots at the origin of the coordinate system show the spatial distributions of the transition moments of the excited molecules.

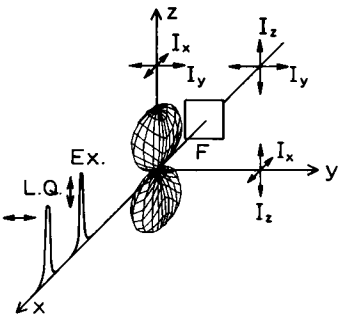

FIGURE 4 Perpendicular two-pulse light quenching. The excited-state population is determined by three polarized intensity components I_x, I_y, and I_z, which can be measured from two different directions of observation. Observation along the x axis requires use of an optical filter F to remove the excitation and quenching beams.

Consider light quenching by a time-delayed quenching pulse. The intensity decreases instantaneously upon arrival of this pulse at time $t = t_d$ (Fig. 1, *middle*). After the quenching pulse, the intensity decays with the same decay time but with decreased amplitude. The intensity decay is unchanged after the pulse because the perturbation is no longer present. If the quenching beam is vertically polarized, the anisotropy decreases upon arrival of the quenching pulse. The anisotropy decreases because the vertically oriented portion of the excited-state population is selectively quenched. If the light quenching beam is horizontally polarized (Fig. 1, *right*), the anisotropy increases because light quenching preferentially depletes the fluorophores oriented along the horizontal axis. In this case, observation of an increase in anisotropy requires observation along an axis other than the y axis (Fig. 2).

The effects of light quenching with a single pulse are illustrated in Fig. 1 (*left*). Such experiments are somewhat more difficult to visualize because both excitation and light quenching occur at the same time. In a one-pulse (one-beam) experiment, the excitation wavelength (λ_{ex}) can be the same or different from the quenching wavelength (λ_q). Such experiments are most conveniently performed with the same laser beam, and we assume $\lambda_{ex} = \lambda_q$ for the one-beam experiments. Light quenching results in a decreased time-zero intensity relative to the absence of light quenching. The time-zero anisotropy is expected to decrease because of photoselective quenching of the vertically oriented fluorophores. The following sections provide a qualitative description of one-beam and two-beam light quenching.

Fluorescence observables in the presence of light quenching

The theoretical description of light quenching is facilitated by the function n (θ, φ, t), which describes the time-dependent angular distribution of the transition moments of the excited molecules (ADTM). This function n (θ, φ, t) represents the density of excited fluorophores, whose transitions are oriented within the angular interval θ to $\theta + d\theta$ and φ to $\varphi + d\varphi$, at time instant t. If this function n (θ, φ, t) is known then the intensity, anisotropy and/or polarization of the emission can be evaluated.

For one-pulse and parallel two-pulse light quenching, the emission field displays cylindrical symmetry. The emission anisotropy is then determined by values of parallel ($I_\parallel$) and perpendicular ($I_\perp$) components of the emission (Fig. 3). These values are usually measured by the same photodetector with two positions of the observation polarizer ($I_\parallel$ and $I_\perp$). In the case of perpendicular two-pulse light quenching, the emission field is not cylindrically symmetrical (Fig. 4) and is compressed into the x-z plane because of preferential quenching of fluorophores oriented along the y axis. The emission anisotropy is then determined by the three polarized components. I_x, I_y, and I_z (Fig. 4), as described by Jablonski (1967). Evaluation of I_x, I_y, and I_z requires measurements carried out from at least two different directions of observation (e.g., y and z, y and x, or x and z). An important conclusion from Fig. 4 is that quenching with horizontally polarized light results in the loss of cylindrical symmetry around the z axis.

In practice it is not convenient to measure the polarized intensities from different directions. For instance, it may be inconvenient to measure the emission from the top of the sample (I_x and I_y) or at small angles relative to the incident beam (I_y and I_z). Fig. 5 shows an alternative method to measure these components. The measurements can be performed twice using the same right angle observation, using vertical, and then horizontal, polarization of the exciting beam, allowing measurements of I_x and I_z and I_x and I_y, respectively.

Depending on polarization of the quenching pulse, the ADTM may or may not display z axis symmetry. For vertically polarized quenching, z axis symmetry of the ADTM is retained, and the function n (θ, φ, t) does not depend on φ (Fig. 3). The time-dependent intensities of the polarized

components of the emission are given by

$$I_{\parallel}(t) = c_1 \int_0^{2\pi} \int_0^{\pi/2} n(\theta, t) \cos^2\theta \sin\theta \, d\theta \, d\varphi, \quad (1)$$

$$I_{\perp}(t) = c_1 \int_0^{2\pi} \int_0^{\pi/2} n(\theta, t) (1 - \cos^2\theta)\cos^2\varphi \sin\theta \, d\theta \, d\varphi, \quad (2)$$

where c_1 is a constant. Equations 1 and 2 allow calculation of the time-resolved anisotropy

$$r(t) = \frac{I_{\parallel}(t) - I_{\perp}(t)}{I_{\parallel}(t) + 2I_{\perp}(t)}. \quad (3)$$

The polarized steady-state intensities, $I_{\parallel}$ and $I_{\perp}$, may be calculated using the time-averaged value of $I_{\parallel}(t)$ and $I_{\perp}(t)$,

$$I_p = c_2 \int_0^{\infty} I_p(t) \, dt, \quad (4)$$

where c_2 is a constant and the subscript p indicates the polarization axis. The steady-state emission anisotropy and polarization can then be calculated as usual from

$$r = \frac{I_{\parallel} - I_{\perp}}{I_{\parallel} + 2I_{\perp}}, \quad (5)$$

$$P = \frac{I_{\parallel} - I_{\perp}}{I_{\parallel} + I_{\perp}}, \quad (6)$$

where the total intensity is given by $I = I_{\parallel} + 2I_{\perp}$.

In cases where the z axis symmetry of the ADTM is not present (Figs. 4 and 5), one can calculate the three different polarized intensities from

$$I_z(t) = c_1 \int_0^{2\pi} \int_0^{\pi/2} n(\theta, \varphi, t)\cos^2\theta \sin\theta \, d\theta \, d\varphi, \quad (7)$$

$$I_x(t) = c_1 \int_0^{2\pi} \int_0^{\pi/2} n(\theta, \varphi, t) (1 - \cos^2\theta)\cos^2\varphi \sin\theta \, d\theta \, d\varphi, \quad (8)$$

$$I_y(t) = c_1 \int_0^{2\pi} \int_0^{\pi/2} n(\theta, \varphi, t) (1 - \cos^2\theta)\sin^2\varphi \sin\theta \, d\theta \, d\varphi. \quad (9)$$

The steady-state intensities of I_x, I_y, and I_z may be calculated using Eq. 4. The lack of axial symmetry of the ADTM requires use of the basic definition of the anisotropy of the radiation field (Jabloński, 1967). This definition, in the presence of light quenching for the coordinate system shown in Figs. 2–5, takes the form

$$r^2 = \frac{(I_x - I_y)^2 + (I_y - I_z)^2 + (I_z - I_x)^2}{2I^2}, \quad (10)$$

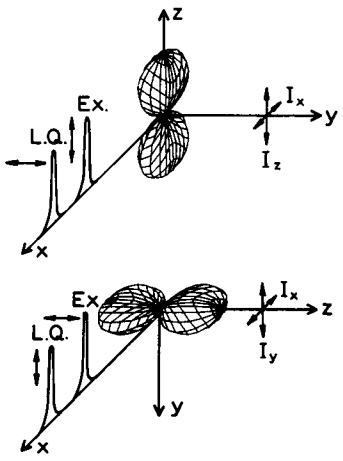

FIGURE 5 Perpendicular two-pulse light quenching. All three components of the polarized intensity can be observed with the same right-angle observation using vertical and horizontal polarization of the exciting beam.

where

$$I = I_x + I_y + I_z \quad (11)$$

In the absence of axial symmetry, evaluation of the emission anisotropy, r, requires observation from two different directions. We use the polarizations P_x, P_y, and/or P_z, defined as

$$P_x = \frac{I_z - I_y}{I_z + I_y}, \quad (12)$$

$$P_y = \frac{I_z - I_x}{I_z + I_x}, \quad (13)$$

$$P_z = \frac{I_y - I_x}{I_y + I_x}. \quad (14)$$

These polarizations may be evaluated when the fluorescence of the sample is observed from the x-, y-, or z direction, respectively. The emission anisotropy given by Eq. 10 can be expressed by any two combinations of the polarizations (12)–(14). For example, when the polarizations P_y and P_z are known, one obtains

$$r^2 = 4 \frac{P_y^2P_z^2 - P_y^2P_z - P_yP_z^2 - P_yP_z + P_y^2 + P_z^2}{(P_yP_z + P_y + P_z - 3)^2}. \quad (15)$$

One-pulse light quenching

We first consider the case where excitation and quenching are caused by the same light pulse (Fig. 3, *top*). Assume that the excitation and quenching pulse appears at time $t = 0$ and the shape of the pulse is described by the function $P(t)$. $P(t)$ is the laser power density (photons/cm^{2}s)) at time t. The incident light is assumed to propagate along the x axis and to be polarized parallel to the z axis. Recalling that we have assumed colinear transition moments, θ is the angle between the electric vector of the incident light and both the absorption and emission transition moments (Fig. 2).

Observation of light quenching in a one-beam experiment requires that the sample absorbs and emits at the same wavelength. This condition is satisfied by fluorophores that display small Stokes' shifts (Lakowicz et al., 1994; Gryczyński et al., 1994), and in some cases of two-photon excitation (Gryczyński et al., 1993). For one-pulse light quenching, the function $n(\theta, \varphi, t)$ displays a z axis symmetry and does not depend on the angle φ, and excitation and quenching occurs within the same laser pulse. If the pulse duration (t_p) is small compared with the excited state lifetime (τ), then during the pulse for times $0 \le t \le t_p$, the excited-state population is described by

$$\frac{dn(\theta, t)}{dt} = P(t)\sigma_a \cos^2\theta\, N - P(t)\sigma_{lq}\cos^2\theta n(\theta, t), \quad (16)$$

where N is the ground-state population, and σ_a and σ_{lq} are the absorption and light quenching cross sections, respectively. The first term on the right represents the rate of excitation, which depends on $\cos^2\theta$ because of the usual photoselection properties of optical transitions (Michl and Thulstrup, 1986). The second term on the right represents light quenching, which depends on laser power density $P(t)$, on $\cos^2\theta$ (Mazurenko, 1973), and on the excited-state population and orientation $n(\theta, t)$. For this reason, the excited-state population does not increase in direct proportion to the incident power, but approaches a maximum value that depends on the relative values of σ_a and σ_{lq}. Note that this apparent "saturation" occurs without the need to consider depopulation of the ground state. Spontaneous decay (characterized by the rate τ^{-1}) is not taken into account in Eq. 16 as being negligible during the very short time scale $0 \le t \le t_p$. However, spontaneous decay is the only process responsible for the depopulation of the excited state after t_p. The time evolution of $n(\theta, t)$ is simply described by

$$\frac{dn(\theta, t)}{dt} = -\frac{1}{\tau} n(\theta, t). \quad (17)$$

Solution of Eqs. 16 and 17 with the initial condition $n(\theta, t = 0) = 0$ leads to the following form for $n(\theta, t)$:

$$n(\theta, t) \quad (18)$$

$$= \begin{cases} N\dfrac{\sigma_a}{\sigma_{lq}}\{1 - \exp[-W(t)\sigma_{lq}\cos^2\theta]\}, \\ \qquad\qquad \text{for} \quad 0 \le t \le t_p, \\ N\dfrac{\sigma_a}{\sigma_{lq}}\{1 - \exp[-W(t_p)\sigma_{lq}\cos^2\theta]\}\left(-\dfrac{t - t_p}{\tau}\right), \\ \qquad\qquad \text{for} \quad t \ge t_p, \end{cases}$$

where

$$W(t) = \int_0^t P(t')\, dt' \quad (19)$$

is the number of photons passing a unit area of the sample until the time t. Equation 18 indicates that for the light quenching by short pulses $n(\theta, t)$ does not depend on the shape of the excitation and quenching pulse, but only on the number of photons that interacted with the sample before the moment of observation. It is also seen from Eq. 18 that the excited-state population at time $t = t_p$ increases sublinearly with pulse energy $W(t_p)$ and tends to a limiting value $N\sigma_a/\sigma_{lq}$. That means that the ground-state population can remain unchanged for any value of the total energy in the laser pulse provided that $\sigma_{lq} \gg \sigma_a$.

In practice, if $t_p \ll \tau$ the emission at times $t \le t_p$ is not observed. The observed emission is then adequately described by the limiting form of the second line of Eq. 18 when $t_p \to 0$

$$n(\theta, t) = n_0(\theta)\exp\left(-\frac{t}{\tau}\right), \quad (20)$$

where

$$n_0(\theta) = N\frac{\sigma_a}{\sigma_{lq}}[1 - \exp(-W_p\,\sigma_{lq}\cos^2\theta)] \quad (21)$$

and $W_p = W(t_p)$. The term $n_0(\theta)$ describes the ADTM created by the combined excitation and quenching pulse, and the term $\exp(-t/\tau)$ is its time evolution after the pulse. The parameter W_p describes the number of photons passing the unit area of the sample during a single pulse. For small values of the product $S_p = W_p\sigma_{lq}$, one can write $\sigma_{lq}^{-1}[1 - \exp(-W_p\sigma_{lq}\cos^2\theta)] \approx W_p\cos^2\theta$, consistent with the common $\cos^2\theta$ photoselection in the absence of light quenching. On the other hand, if the value of S_p becomes large then for most values of the angle θ (except for $\theta \approx \pi/2$) one obtains $\exp(-S_p\cos^2\theta) \ll 1$, and $n_0(\theta) \approx N\sigma_a/\sigma_{lq}$. This means that with S_p tending to infinity the ADTM becomes more and more spherical.

The effect of laser power or S_p on the excited-state population is shown in Fig. 6. At low laser power, the usual $\cos^2\theta$ distribution is obtained (*left*), and the anisotropy is 0.4 (the polarization is 0.5). At higher laser power ($S_p = 3$), the excited-state distribution becomes compressed along the z

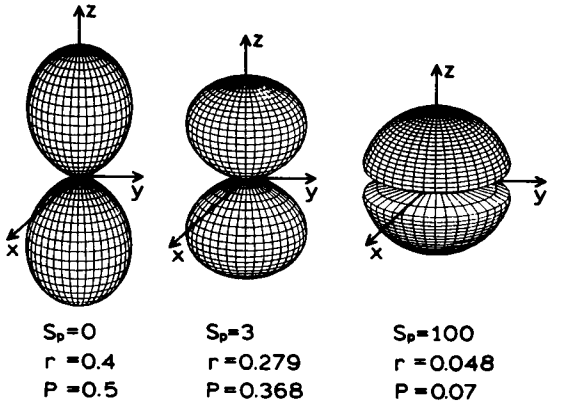

FIGURE 6 Effect of one-pulse light quenching on the excited-state population $n_0(\theta)$ (Eq. 21) for different values of S_p. The plots have been approximately normalized to the same volume. The anisotropy and polarization were calculated from Eqs. 5, 6, 22, and 23.

axis, and the anisotropy and polarization decrease (*middle*). At still higher amounts of light quenching (S_p = 100), the excited-state distribution becomes nearly spherical, suggesting that the anisotropy approaches zero (*right*). We note that the effect of decreasing anisotropy is not the result of ground-state depletion. The excited-state orientation distribution becomes compressed along the z axis because of selected quenching of fluorophores oriented along this axis during the laser pulse. The excited-state population remains symmetrical around the z axis because of z axis symmetry of the electrical vector of the incident light.

To understand better the parameter S_p in light quenching, we note that S_p is equal to the average number of photons passing the light quenching cross section of the fluorophore (σ_{1q}) during the quenching pulse. Because the laser repetition rate is assumed low compared with rate of spontaneous decay, S_p can also be understood as a number of photons during the fluorophore's mean lifetime.

Effect of One-Pulse Quenching on Steady-State Intensity and Anisotropy

Calculation of the steady-state intensity and anisotropy requires calculation of the intensities of the polarized components of the emission. For a single beam experiment using Eqs. 1, 2, 4, and 20, and using the substitution $\cos(\theta) = x$, one obtains

$$I_{\parallel} = c_3 N \frac{\sigma_a}{\sigma_{1q}} \int_0^1 [1 - \exp(-S_p x^2)] x^2 \, dx, \qquad (22)$$

$$I_{\perp} = \frac{c_3}{2} N \frac{\sigma_a}{\sigma_{1q}} \int_0^1 [1 - \exp(-S_p x^2)](1-x^2) \, dx, \qquad (23)$$

where $c_3$is a constant. These integrals can be evaluated numerically. The dependence of $I_{\parallel}$, $I_{\perp}$, the total intensity $I = i_{\parallel} + 2I_{\perp}$ and the steady-state anisotropy on the parameter S_p, is shown by the dotted lines in Fig. 7. The emission intensities are normalized so that $I \to 1$ when $S_p \to \infty$. The maximum value of the intensity depends on the number of fluorophores in the ground state and on the ratio of σ_a/σ_{1q}. The values of the intensities of the polarized components may be used to calculate the steady-state anisotrophy (Eq. 5). In the limit when $S_p \to \infty$ both polarized components, $I_{\parallel}$ and $I_{\perp}$ tend to the same finite value, which is ⅓ of the total intensity I. This causes the emission anisotropy to approach zero at high values of S_p.

The extent of quenching can be described by the parameter $Q_p = I_0/I$, where $I_0 = I_{\parallel}^0 + 2I_{\perp}^0$ and $I = I_{\parallel} + 2I_{\perp}$ are the fluorescence intensities at the same incident power, in the absence and presence of light quenching, respectively. In the case of one-pulse quenching the values of $I_{\parallel}^0$ and $I_{\perp}^0$ can be found from Eqs. 22 and 23 by setting $\sigma_{1q} = 0$. The value of

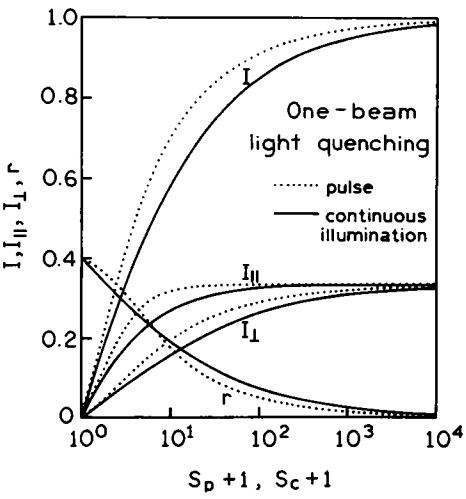

FIGURE 7 Polarized intensities, $I_{\parallel}$ and $I_{\perp}$, total intensity, $I = I_{\parallel} + 2I_{\perp}$, and anisotropy, r, of the emission for increasing values of S_p (*dotted lines*) or S_c (*solid lines*). The dotted lines are for one-pulse light quenching (Eqs. 22 and 23) and the solid lines are for continuous illumination (Eqs. 28 and 29). The total intensities are normalized so that $I \to 1$ when $S_p \to \infty$ or $S_c \to \infty$, respectively.

Q_p is then calculated using

$$Q_p = \frac{I_0}{I} = \left(\frac{3}{S_p} \int_0^1 [1 - \exp(-S_p x^2)] \, dx \right)^{-1}. \qquad (24)$$

The relative values of the light quenching cross sections can thus be found from a plot of I_0/I versus laser power. For small values of S_p, Eq. 24 can be approximated by

$$Q_p = \frac{I_0}{I} = 1 + \frac{3}{10} S_p, \qquad (25)$$

indicating Stern-Volmer behavior for one-pulse light quenching at low intensities of the incident light or at small values of the light quenching cross section. The exact (Eq. 24) and approximate (Eq. 25) dependence of Q_p on laser power are shown in Fig. 8. A linear Stern-Volmer plot is seen for pulse light quenching when $S_p < 1$. The slope of the quenching plot slowly changes with increasing values of S_p. In the limit when $S_p \to \infty$, Eq. 24 reduces to $Q_p = ⅓S_p$.

Light quenching by continuous illumination

It is interesting to compare the expected effects for quenching by pulses (one-beam) and by illumination with a constant intensity light source. Instead of pulsed illumination, a continuous (c) laser beam of the power density P propagates along the x axis and is polarized parallel to the z axis (Fig. 2). The excited-state population is then described by

$$\frac{dn(\theta, t)}{dt} = P\sigma_a \cos^2\theta \, N - \left[\frac{1}{\tau} + P\sigma_{1q} \cos^2\theta \right] n(\theta, t). \qquad (26)$$

Compared with Eq. 16, Eq. 26 contains the rate of spontaneous decay, τ^{-1}, which cannot be neglected on this longer

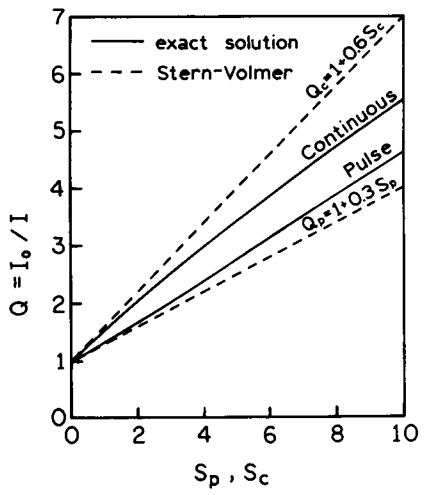

FIGURE 8 Amount of quenching for one-beam pulse (Q_p) and continuous (Q_c) illumination for increasing values of S_p or S_c. The solid lines represent expressions (24) and (30), and the dashed lines represent the respective Stern-Volmer-type approximations.

timescale. Under the steady-state conditions, the time derivative in Eq. 26 equals zero and the function $n(\theta, t)$ approaches its limiting, time-independent value $n_c(\theta)$

$$n_c(\theta) = N\frac{P\tau\sigma_a\cos^2\theta}{1 + P\tau\sigma_{lq}\cos^2\theta} = N\frac{\sigma_a}{\sigma_{lq}}\frac{S_c\cos^2\theta}{1 + S_c\cos^2\theta}, \quad (27)$$

where $S_c = P\tau\sigma_{lq}$. A physical meaning of the parameter S_c is the average number of photons passing the light quenching cross section of the fluorophore during the fluorophore's mean lifetime. The excited-state population $n_c(\theta)$ for three different values of S_c are shown in Fig. 9. For small values of S_c, one obtains $n_c(\theta) \approx NP\tau\sigma_a\cos^2\theta$, which again is the usual $\cos^2\theta$ distribution of excited fluorophores. For larger values of $S_c \gg 1$, then $n_c(\theta) = N\sigma_a/\sigma_{lq}$. This means that, as for one-pulse light quenching, the shape of the ADTM tends

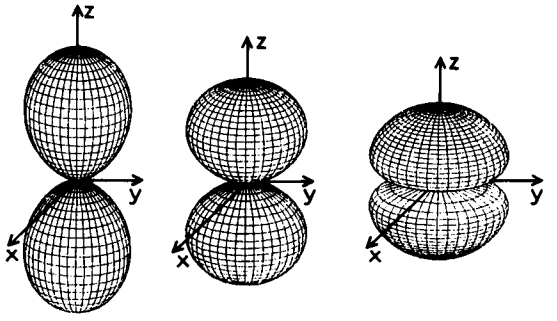

FIGURE 9 Effect of light quenching on the excited state population $n_c(\theta)$ (Eq. 27) for a continuous illumination and increasing values of the parameter S_c. The plots have been approximately normalized to the same volume. The corresponding values of anisotropy and polarization have been calculated from Eqs. 5, 6, 28, and 29.

to a sphere, and the anisotropy tends towards zero, as the intensity of the incident power tends to infinity.

Effect of continuous illumination on the steady-state intensity and anisotropy

The steady-state intensities in the presence of continuous light quenching can be calculated by introducing Eq. 27 into Eqs. 1 and 2, use of Eq. 4, and substituting $\cos^2\theta = x$, yielding

$$I_\parallel = c_3 N S_c \frac{\sigma_a}{\sigma_{lq}} \int_0^1 \frac{x^4}{1 + S_c x^2}\,dx, \quad (28)$$

$$I_\perp = \frac{c_3}{2} N S_c \frac{\sigma_a}{\sigma_{lq}} \int_0^1 \frac{x^2(1 - x^2)}{1 + S_c x^2}\,dx, \quad (29)$$

in agreement with the results of Mazurenko (1973). The intensities of the polarized components obtained from Eqs. 28 and 29 can be used to calculate the steady-state anisotropy (Eq. 5). The solid lines in Fig. 7 show the values of $I_\parallel$, $I_\perp$, the total intensity $I = I_\parallel + 2I_\perp$, and the steady-state anisotropy for light quenching by continuous illumination. The emission intensities are normalized so that $I \to 1$ when $S_c \to \infty$. For intermediate values of S_p and S_c (<8), the steady-state intensities for continuous illumination are lower than for pulse excitation. This indicates that continuous illumination is more effective in light quenching for comparable values of S_c and S_p. For continuous illumination, the excited-state population reaches its constant maximum value during illumination. In contrast, for pulse excitation the excited-state population increases monotonically within the pulse from zero at time $t = 0$ to its maximum at $t = t_p$. This results in a lower time-averaged value of the excited-state population and, hence, fewer excited-state molecules to be quenched.

Both pulsed and continuous light quenching results in a decreased steady-state anisotropy. It is interesting to note that the decrease in anisotropy is initially larger for continuous illumination for smaller values of S_p (Fig. 7). For values of $S_p(S_c)$ greater than 10, pulsed illumination becomes more effective. The intersection of anisotropy curves in Fig. 7 is a result of two different behaviors in the one-pulse light quenching for different values of the parameter S_p. For low values of S_p, the higher steady-state anisotropy for pulse quenching results from of the mechanism described above to explain the differences in the intensities. The smaller amounts of quenching for pulsed excitation result in smaller changes in the anisotropy. For high values of S_p, the steady-state anisotropy for pulse quenching is lower than that for continuous illumination. For high values of S_p, the increase of the excited-state population during the light pulse becomes limited by the process of light quenching as can be seen from the first line of Eq. 18. This leads to comparable amounts of quenching for both kinds of excitation. However, comparable amounts of quenching do not have to lead to comparable anisotropies. For pulse excitation and quenching, practically all observed luminescence is emitted by the excited-state population, which has been modified by the

process of light quenching. For continuous illumination, this modification of the excited-state population continues throughout the intensity decay. However, a significant fraction of the luminescence may be emitted from the partially changed population, resulting in higher anisotropy at comparable intensities.

The extent of light quenching by the continuous illumination can be described by the parameter $Q_c = I_0/I$, where $I_0 = I_\parallel^0 + 2I_\perp^0$ and $I = I_\parallel + 2I_\perp$ are the fluorescence intensities at the same incident power, in the absence and presence of light quenching, respectively. Computationally, the values of $I_\parallel^0$ and $I_\perp^0$ can be found from Eqs. 28 and 29 by setting $\sigma_{lq} = 0$ (note that in these equations σ_{lq} is also involved in the parameter S_c). The value of Q_c is then calculated using

$$Q_c = \frac{I_0}{I} = \left(3\int_0^1 \frac{x^2}{1 + S_c x^2}\,dx\right)^{-1} \tag{30}$$

For very small values of S_c, Eq. 30 reduces to (Lakowicz et al., 1994)

$$Q_c = \frac{I_0}{I} = 1 + \frac{6}{10}S_c. \tag{31}$$

Plots of Eqs. 30 and 31 are shown in Fig. 8. The initial slope of Eq. 31 for continuous quenching is twofold higher than for pulsed illumination (Eq. 25). This result reflects the fact that the total excited-state population is present during continuous illumination. In contrast, for one-pulse light quenching, the excited-state population increases from zero to the maximum value during the pulse, and on average only half of the excited fluorophores are available for light quenching. As the value of S_c increases, the slope of quenching plot continuously decreases. In the limit when $S_c \to \infty$, Eq. 30 reduces to $Q_c = \frac{1}{3}S_c$, as for one-pulse quenching.

Two-pulse light quenching

We now consider the second class of light quenching experiments in which the sample is illuminated with two different light pulses (Fig. 1, *middle* and *right*). The pulses are linearly polarized and separated by a delay time t_d. In this case the wavelengths, intensity, and arrival time of the two pulses can be independently controlled. We assume that the fluorophore's cross section for light quenching at the excitation wavelength of the first pulse is negligibly small compared with the cross section for light absorption. The cross section for light quenching at wavelength of the second pulse is assumed to be much higher than the cross section for light absorption at this wavelength. Thus, the first and second pulse are understood as the excitation and quenching pulse, respectively. As for one-pulse light quenching, we assume that the durations of both pulses, t_{p1} and t_{p2}, are small compared with the excited-state lifetime. The shape of the first pulse is described by the function $P_1(t)$ and the shape of the second pulse by the function $P_2(t)$. Within the time of the first pulse, (which is assumed to propagate along the direction of the x axis and to be polarized parallel to the z axis), the time evolution of the angular distribution of the transition dipoles of the excited molecules (ADTM) is described by

$$\frac{dn(\theta, t)}{dt} = P_1(t)\sigma_a\cos^2\theta N. \tag{32}$$

Equation 32 implies that the time-zero distribution immediately after the excitation pulse is given by

$$n_0(\theta) = NW_{p1}\sigma_a\cos^2\theta, \tag{33}$$

where

$$W_{p1} = \int_0^{t_{p1}} P_1(t)\,dt. \tag{34}$$

The shape of the time-zero distribution displays z axis symmetry and is determined by $\cos^2\theta$ due to photoselection. Further temporal evolution of the ADTM depends on the relationship between the lifetime τ and the correlation time Θ characterizing the rate of the rotational diffusion in the sample. For the present discussion, we assume that the correlation time is long and that the effects of the rotational diffusion can be neglected. Hence, only effect before arrival of the second pulse is a decrease of the excited-state population caused by the spontaneous decay, which is not dependent on the orientation of the molecule. Thus, for times $0 < t \le t_d$ after the excitation pulse and before the quenching pulse, we have

$$n(\theta, t) = n_0(\theta)\exp\left(-\frac{t}{\tau}\right). \tag{35}$$

For two-pulse light quenching, the propagation and/or polarization direction of the second pulse may be arbitrarily oriented relative to the direction of the first pulse. This implies that the ADTM may not display the z axis symmetry after the quenching pulse passes through the sample. Therefore, the distribution has to be described using two angles, θ and φ (Fig. 2). For times $t_d \le t \le t_d + t_{p2}$, during the quenching pulse, the excited-state population is described by

$$\frac{dn(\theta, \varphi, t)}{dt} = -P_2(t)\sigma_{lq}\Psi(\theta, \varphi)n(\theta, \varphi, t), \tag{36}$$

where the function $\Psi(\theta, \varphi)$ returns the squared value of the projection of the unit vector, describing the direction of the electrical field in the quenching pulse on the direction of the molecular emission moment described by the angles θ and φ.

In two-pulse light quenching, there are two basic orientations of the electrical field in the quenching pulse. In parallel quenching, the polarizations of the excitation and quenching pulse are parallel; and in perpendicular quenching, the polarization directions are perpendicular. In both cases, the propagation direction of the quenching pulse is chosen to be colinear with the propagation direction of the

excitation pulse. Thus, we have

$$\Psi(\theta, \varphi) = \begin{cases} \cos^2\theta, & \text{for parallel quenching,} \\ \sin^2\theta\sin^2\varphi, & \text{for perpendicular quenching.} \end{cases} \tag{37}$$

Note, that because of the assumed z axis symmetry of the ADTM immediately before quenching, the result of quenching is the same for any propagation direction of the quenching pulse, provided the direction is in the x-y plane. The initial condition of Eq. 36 may be obtained by setting $t = t_d$ in Eq. 35. This condition describes the shape of the ADTM immediately before (b) arrival of the quenching pulse

$$n_b(\theta, \varphi) = n(\theta, t_d) = n_0(\theta)\exp\left(-\frac{t_d}{\tau}\right). \tag{38}$$

Solution of Eq. 36 with the initial condition (38) yields for $t_d \le t \le t_d + t_{p2}$

$$n(\theta, \varphi, t) = n_0(\theta)\exp[-W_2(t)\sigma_{lq}\Psi(\theta, \varphi)]\exp\left(-\frac{t}{\tau}\right), \tag{39}$$

where

$$W_2(t) = \int_{t_d}^{t} P_2(t)\, dt. \tag{40}$$

Based on Eq. 39 and recalling that $t_{p2} \ll \tau$, one obtains the ADTM immediately after (a) the quenching pulse

$$n_a(\theta, \varphi) = n_0(\theta)\exp[-W_{p2}\sigma_{lq}\Psi(\theta, \varphi)]\exp\left(-\frac{t_d}{\tau}\right), \tag{41}$$

where $W_{p2} = W_2(t_d + t_{p2})$. After the quenching pulse for times $t > t_d + t_{p2}$, the excited-state population given by Eq. 41 decays uniformly for all dipole orientations caused by the process of spontaneous decay,

$$n(\theta, \varphi, t) = n_0(\theta)\exp[-S_{p2}\Psi(\theta, \varphi)]\exp\left(-\frac{t}{\tau}\right), \tag{42}$$

where $S_{p2} = W_{p2}\sigma_{lq}$.

The relative change of the excited-state population caused by the quenching pulse can be described by the parameter $q = (n_b - n_a)/n_b$, where n_b and n_a are the total number of excited molecules immediately before and after the quenching pulse. The number n_b and/or n_a is defined as an integral (over all values of θ and φ) of the function $n(\theta, \varphi, t)$ for $t = t_d$ and/or $t = t_d + t_{p2}$, respectively. These values should be distinguished from the number N, introduced in Eq. 16 to denote the ground-state population. The value of $n(\theta, \varphi)$ represents the density of the excited-state fluorophores, whose transitions are oriented within the angular interval θ to $\theta + d\theta$ and φ to $\varphi + d\varphi$, whereas the numbers n_b and n_a correspond to the total numbers of the excited molecules. Based on Eqs. 33, 38, and 41, one obtains

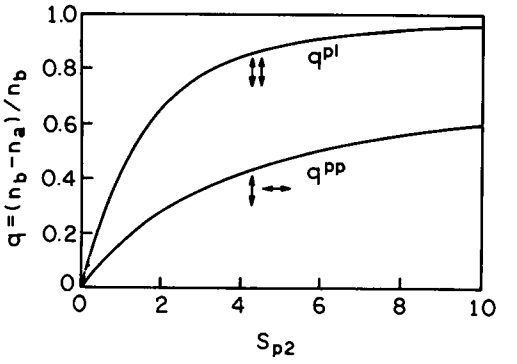

FIGURE 10 Relative change of the excited state population (Eq. 43) versus S_p for parallel (q^{pl}) and perpendicular (q^{pp}) light quenching. The ADTM immediately before light quenching is described by Eq. 33.

$$q = \frac{n_b - n_a}{n_b} \tag{43}$$

$$= 1 - \frac{3}{2\pi}\int_0^{2\pi}\int_0^{\pi/2} \cos^2\theta \exp[-S_{p2}\Psi(\theta, \varphi)]\sin\theta\, d\theta\, d\varphi.$$

Plots of the parameter q for parallel (pl) and perpendicular (pp) light quenching versus the parameter $S_{p2} = W_{p2}\sigma_{lq}$ are shown in Fig. 10. The significant difference between q^{pl} and q^{pp} is caused by the initial distribution $n_0(\theta)$ (Eq. 33), which is more highly oriented along the z axis and provides higher efficiency for parallel quenching. As shown below, the preferential quenching based on $\cos^2\theta$ photoselection provides the opportunity to change the steady-state and time-resolved anisotropy by time delayed quenching pulses.

Summarizing this section, one can say that for short excitation and quenching pulses, the ADTM is satisfactorily described by the function that has a jump at time $t = t_d$

$$n(\theta, \varphi, t) \tag{44}$$

$$= \begin{cases} n_0(\theta)\exp\left(-\frac{t}{\tau}\right), & \text{for } 0 < t \le t_d, \\ n_0(\theta)\exp[-S_{p2}\Psi(\theta, \varphi)]\exp\left(-\frac{t}{\tau}\right), & \text{for } t > t_d, \end{cases}$$

where $n_0(\theta)$ and $\Psi(\theta, \varphi)$ are given by Eqs. 33 and 37, respectively. The jump is a result of light quenching and is described by the term $\exp[-S_{p2}\Psi(\theta, \varphi)]$. The initial z axis symmetry of the ADTM remains unchanged only if the polarizations of the excitation and quenching pulse are parallel.

Effect of two-pulse light quenching on the steady-state intensity and anisotropy

The effect of a time-delayed quenching pulse on the steady-state intensity and anisotropy depends on polarization of the quenching pulse. For parallel (pl) quenching, the polarized

components of the emission can be obtained from Eqs. 1, 2, 4, 33, and 44, yielding

$$I_{\parallel}^{pl} = \frac{c_3}{5} NW_{pl}\sigma_a \left\{1 - \exp\left(-\frac{t_d}{\tau}\right)\left[1 - 5\int_0^1 \exp(-S_{p2}x^2)x^4\,dx\right]\right\}, \tag{45}$$

$$I_{\perp}^{pl} = \frac{c_3}{15} NW_{pl}\sigma_a \left\{1 - \exp\left(-\frac{t_d}{\tau}\right)\left[1 - \frac{15}{2}\int_0^1 \exp(-S_{p2}x^2)(1-x^2)x^2\,dx\right]\right\}. \tag{46}$$

The amount of quenching of the total emission is given by

$$Q_{2p}^{pl} = \frac{I_0}{I} = \left\{1 - \exp\left(-\frac{t_d}{\tau}\right)\left[1 - 3\int_0^1 \exp(-S_{p2}x^2)x^2\,dx\right]\right\}^{-1}. \tag{47}$$

For perpendicular (pp) quenching the z axis is no longer a symmetry axis, and $I_x \neq I_y$. The values of I_x, I_y, and I_z can be obtained from Eqs. 7–9, 4, 33, and 44, yielding

$$I_z^{pp} = \frac{c_3}{5} NW_{pl}\sigma_a \left\{1 - \exp\left(-\frac{t_d}{\tau}\right)\left[1 - \frac{5}{2\pi}\int_0^{2\pi}\int_0^1 \exp(-S_{p2}(1-x^2)\sin^2\varphi]x^4\,dx\,d\varphi\right]\right\}, \tag{48}$$

$$I_x^{pp} = \frac{c_3}{15} NW_{pl}\sigma_a \left\{1 - \exp\left(-\frac{t_d}{\tau}\right)\left[1 - \frac{15}{2\pi}\int_0^{2\pi}\int_0^1 \exp[-S_{p2}(1-x^2)\sin^2\varphi](1-x^2)x^2\cos^2\varphi\,dx\,d\varphi\right]\right\}, \tag{49}$$

$$I_y^{pp} = \frac{c_3}{15} NW_{pl}\sigma_a \left\{1 - \exp\left(-\frac{t_d}{\tau}\right)\left[1 - \frac{15}{2\pi}\int_0^{2\pi}\int_0^1 \exp[-S_{p2}(1-x^2)\sin^2\varphi](1-x^2)x^2\sin^2\varphi\,dx\,d\varphi\right]\right\}. \tag{50}$$

The total amount of quenching is given by

$$Q_{2p}^{pp} = \left\{1 - \exp\left(-\frac{t_d}{\tau}\right)\left[1 - \frac{3}{2\pi}\int_0^{2\pi}\int_0^1 \exp[-S_{p2}(1-x^2)\sin^2\varphi]x^2\,dx\,d\varphi\right]\right\}^{-1}. \tag{51}$$

These expressions allow calculation of the emission anisotropy or polarization for values of S_{p2}. Before describing these effects, it is important to recognize that the change in anisotropy or polarization will depend strongly on the delay time t_d. The steady-state polarization is an average of the values before and after the light quenching pulse, and thus depends on t_d. As the delay time is increased, a larger fraction of the emission occurs from the initial unperturbed excited-state population. Consequently, the largest effects occur when the quenching pulse arrives immediately after the excited pulse, that is, for a delay time of zero. At first glance, this appears to be the same as the one-beam experiment in which the pulses arrive simultaneously at the sample. However, these cases are quite different. Recall that fluorescence lifetime are typically in the range of 1–10 ns, whereas it is relatively easy to obtain laser pulses near 5 ps in width. Hence, in practice one can readily obtain a delay time near zero relative to the ns fluorescence lifetime, and still have the quenching pulse arrival after the excitation pulse. We refer to this case as $t_d = 0$, where it is understood that the quenching pulse arrives after the excitation pulse.

Suppose the excitation and quenching pulses are both vertically polarized and the quenching pulse arrives immediately after excitation, that is, $t_d = 0$. The excited-state populations are shown in Fig. 11 for no light quenching ($S_{p2} = 0$) and for

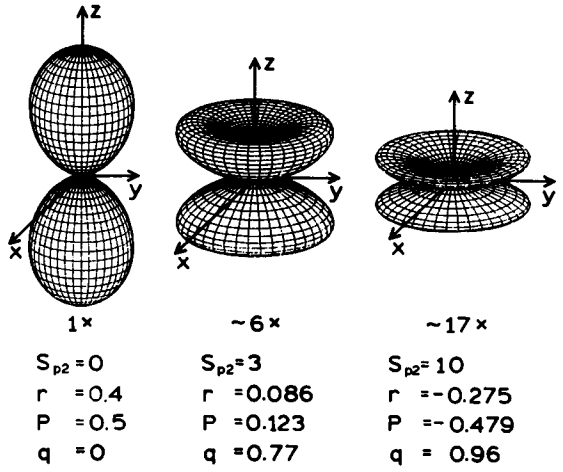

FIGURE 11 Effect of a time-delayed quenching pulse on the excited-state population (Eq. 41). The quenching pulse is polarized parallel to the z axis. Plots for $S_{p2} = 3$ and $S_{p2} = 10$ are magnified approximately 6 and 17 times, respectively. The corresponding values of r, P, and q have been calculated from Eqs. 5, 6, 43, 45, and 46, with $t_d = 0$

increasing values of $S_{p2} = 3$ or 10. The time-delayed quenching pulse has the remarkable effect of depleting the excited-state population along the z axis, resulting in the unusual shapes shown in Fig. 11. Because of the selective depletion along the z axis, the polarization and anisotropy become negative for larger values of S_{p2}.

Remarkably different effects on the excited-state population are expected for a perpendicular quenching pulse (Fig. 12). In the case of the initial $\cos^2\theta$ distribution (*left*) is selectively depleted along the y axis, resulting in a flattened shape. Consequently, the excited-state population is not symmetrical around the z axis and the measured polarization depends upon the direction of observation. For instance, perpendicular light quenching results in a more highly oriented population when observed from the x- or z directions, but no change is observed when using the usual right angle observation along the y axis.

The effects of parallel (pl) and perpendicular (pp) light quenching on the observed polarization are summarized in Fig. 13. For parallel light quenching, the initial polarization of 0.5 decreases to -1.0 as the amount of light quenching increases. It is valuable to note that negative polarization values occur for just 10-fold quenching, so that the effects of light quenching can be readily observed with a reasonable amount of quenching. Also shown in Fig. 13 are the changes in polarization caused by one-pulse light quenching. In this case, the polarization decreases from 0.5 to zero, reflecting the spherical distribution shown in Fig. 6. Two-pulse light quenching is thus seen to result in larger changes in polarization than one-pulse light quenching.

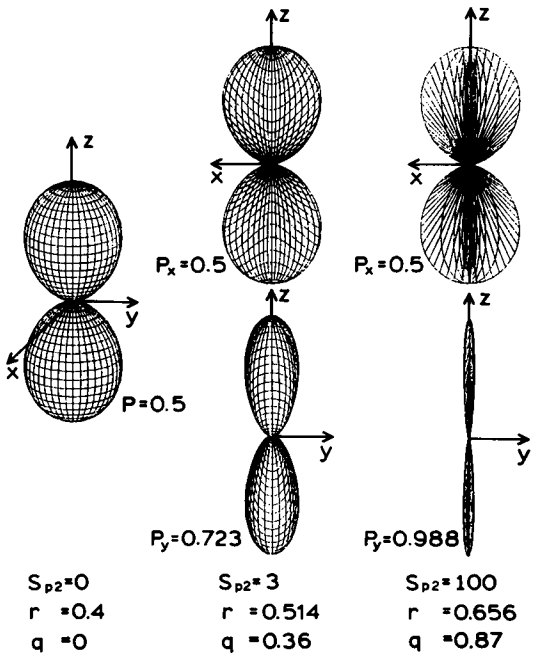

FIGURE 12 Effect of a time-delayed quenching pulse on the excited-state population (Eq. 41). The quenching pulse is polarized along the y axis. In this case, the excited-state population is not symmetrical around the z axis. The corresponding values of r, P_x, P_y, and q have been calculated from Eqs. 10, 12–14, 43, 48, and 49, with $t_d = 0$.

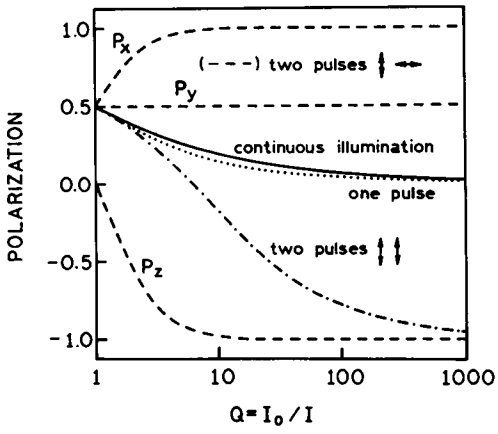

FIGURE 13 Emission polarization in the presence of light quenching. For one-pulse quenching (·····), P was calculated from Eqs. 6, 22, and 23; for parallel (↕ ↕) two-pulse quenching (–·–·–)—from Eqs. 6, 45, and 46, and for perpendicular (↕ ↔) two-pulse quenching (– – – –)—from Eqs. 12, 14 and 48–50. The solid line shows the values of P calculated from Eqs. 6, 28, and 29 for continuous illumination. The values of Q were found from Eqs. 24, 30, 47, or 51. The delay time t_d was set equal to zero in the calculations.

For perpendicular quenching, the polarization depends on the direction of observation (Fig. 13). When observed along the y axis, there is no change in polarization, as can be seen from the excited-state distribution in Fig. 12 (*top, right*). If the emission is observed at a small angle from the propagation of the quenching beam, the polarization (P_x) increases from 0.5 to 1.0. When observed along the z axis, the polarization in the absence of light quenching is zero because of the initial symmetry around this axis. As the extent of light quenching increases, P_z approaches -1.0. It is apparent from Fig. 13 that a wide range of polarizations can be obtained with time-delayed quenching pulses.

Fig. 13 also compares the effects of continuous (*solid line*) and one-pulse (*dotted line*) light quenching for increasing values of Q. In both cases, the polarization approaches zero for high amounts of light quenching. However, one-pulse quenching is somewhat more effective in decreasing the polarization as the entire emission is from the perturbed population, whereas for continuous illumination some emission occurs from the unaffected fluorophores.

Effects of the time-delay (t_d) on the steady-state intensity and anisotropy

In the preceding section, we discussed the excited-state population when the quenching pulse arrived immediately after the excitation pulse. We now consider the effects of the time-delay between these two pulses on the steady-state intensity and polarization. The effect of the quenching pulse depends upon the number of excited-state molecules. Consequently, for the same power in the quenching pulse, the amount of quenching or change in polarization is expected to decrease as the time-delay becomes larger relative to the excited-state lifetime. This effect is shown in Fig. 14 for parallel (*top*) and perpendicular (*bottom*) quenching pulses.

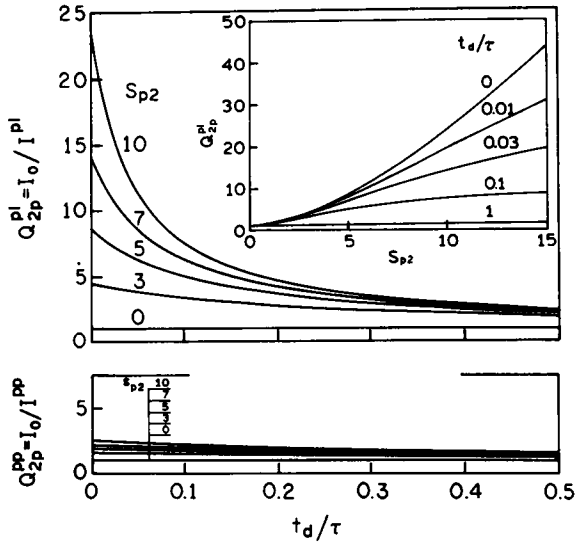

FIGURE 14 Two-pulse light quenching. Effect of the delay time t_d and the parameter $S_{p2} = W_{p2}\sigma_{1q}$ on the amount of quenching Q_{2p}^{pl}, (Eq. 47) and Q_{2p}^{pp} (Eq. 51) for parallel (*top*) and perpendicular (*bottom*) polarized pulses, respectively.

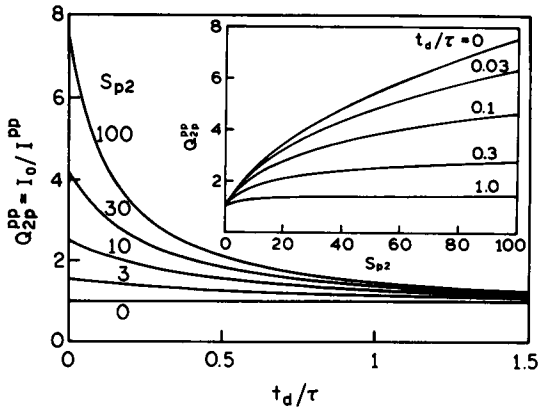

FIGURE 15 Two-pulse perpendicular light quenching. Effect of the delay time t_d and the parameter $S_{p2} = W_{p2}\sigma_{1q}$ on the amount of quenching Q_{2p}^{pp}, (Eq. 51).

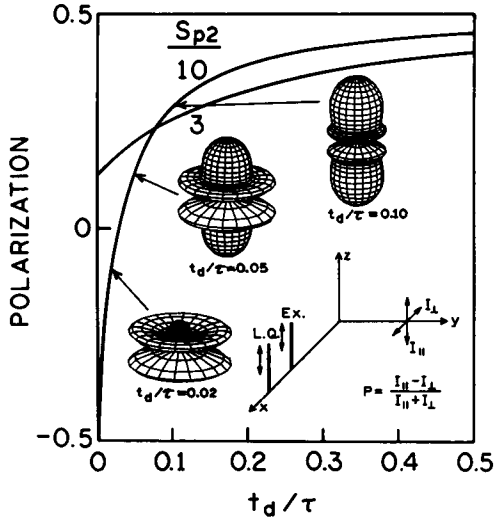

FIGURE 16 Effect of a time-delay parallel quenching pulse on the emission polarization. Values of polarization (P) were calculated from Eqs. 6, 45, and 46. The polar plots show the combined steady-state, excited-state populations calculated from Eq. 52 for $S_{p2} = 10$ and different time delays of the quenching pulse. The arrows indicate the points on the anisotropy curve where the given shape of the ADTM applies.

For clarity, we note that the $Q = I_0/I$ is the ratio of the steady-state emission in the absence and presence of quenching, respectively. As the time-delay increases, the amount of quenching decreases in an approximate exponential manner. There are fewer molecules in the excited-state at longer delay times and, hence, fewer molecules to quench. This is a unique feature of light quenching, as compared with collisional quenching, which starts immediately after excitation. In the case of light quenching, the quenching event can be delayed to allow time for rotational diffusion, spectral relaxation, or other excited-state processes.

Examination of Fig. 14 reveals that the delayed quenching pulse is much more effective when polarized parallel to the excitation pulse (*top*). At comparable laser power and time delays, one expects relatively little quenching for a perpendicularly polarized quenching pulse (*bottom*). However, quenching can be accomplished at higher laser power, as shown in Fig. 15. It is important to note that the extent of quenching (I_0/I) of the polarized components is not linear with laser power (Figs. 14 and 15, *insets*).

The orientation-dependent effects of the quenching pulses on the excited-state population result in changes in polarization. Once again, the effect depends upon the time-delay (t_d) because the steady-state values are the intensity-weighted average of the polarization before and after the quenching pulse. The effect of t_d for parallel and perpendicular pulses is shown in Figs. 16 and 17, respectively. The largest change in polarization is seen for the shortest delay times. These calculations can guide the design of future experiments on light quenching. For instance, observation of a change in the polarization from positive to negative values can only be accomplished with short time delays ($t_d/\tau < 0.03$) and for high amounts of quenching ($S_{p2} \geq 4$, Fig. 16). For delay times longer than 20% of the lifetime ($t_d/\tau > 0.2$), one can expect only modest changes in the polarization for reasonable values of S_{p2}. Experimentally, this is an advantage because it is typically easier to obtain short time delays between pulses, because long delays can require inconveniently long light paths.

To understand the polarization of the fluorescence resulting from pulsed excitation and steady state, observation is useful to calculate the steady-state ADTM. This excited-state population is defined as a weighted combination of ADTMs observed before and after the quenching pulse

$$n(\theta, \varphi) = n_1(\theta) + n_2(\theta, \varphi), \tag{52}$$

where (see Eqs. 33 and 41)

$$n_1(\theta) = w_1 \cos^2\theta, \tag{53}$$

$$n_2(\theta, \varphi) = w_2 \cos^2\theta \exp[-S_{p2}\Psi(\theta, \varphi)]. \tag{54}$$

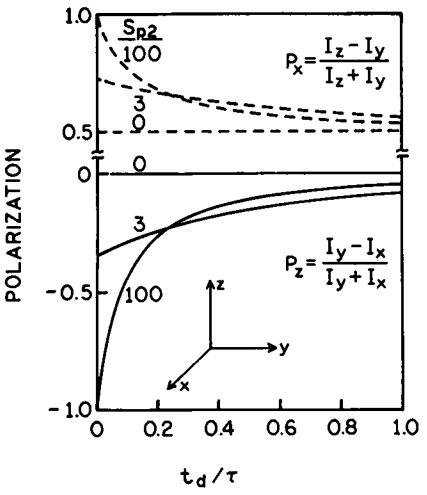

FIGURE 17 Effect of a time-delay perpendicular quenching pulse on the emission polarization. Values of polarization were calculated from Eqs. 12, 14, and 48–50. The dashed (P_x) and solid (P_z) lines show the polarization observed from x- and z direction, respectively.

The weights w_1 and w_2 are selected so that the total numbers of the excited molecules in the ADTMs, calculated from

$$n_k = \int_0^{2\pi} \int_0^{\pi/2} n_k(\theta, \varphi) \sin\theta \, d\theta \, d\varphi \tag{55}$$

are proportional to the respective contributions of the unquenched and quenched emission in the steady-state intensity. These contributions can be calculated as

$$I_1 = \int_0^{t_d} I_1(t) \, dt, \qquad I_2 = \int_{t_d}^{\infty} I_2(t) \, dt, \tag{56}$$

where the intensity decays $I_1(t)$ and $I_2(t)$ are found from the equation describing the total fluorescence intensity, resulting from Eqs. 7–9

$$\begin{aligned} I_k(t) &= I_{kx}(t) + I_{ky}(t) + I_{kz}(t) \\ &= c_1 \int_0^{2\pi} \int_0^{\pi/2} n_k(\theta, \varphi, t) \sin\theta \, d\theta \, d\varphi. \end{aligned} \tag{57}$$

To calculate I_1 or I_2, the function $n_k(\theta, \varphi, t)$ in Eq. 57 should be expressed by Eq. 35 or Eq. 42, respectively. Comparison of the so calculated steady-state contributions I_1 and I_2 with Eq. 55 yields the coefficients w_1 and w_2

$$w_1 = 1 - \exp\left(-\frac{t_d}{\tau}\right), \tag{58}$$

$$w_2 = \exp\left(-\frac{t_d}{\tau}\right). \tag{59}$$

The shapes of the calculated steady-state ADTMs (Eq. 52) are shown in Fig. 16 for $S_{p2} = 10$ and different values of the time delay t_d/τ. At a short delay term ($t_d/\tau = 0.02$), the ADTM is a flattened disk, resulting in a steady-state polarization of -0.086. As the delay time is increased to $t_d/\tau = 0.05$, one observes an increase in the unquenched ($\cos^2\theta$) distribution. At a still longer delay time ($t_d/\tau = 0.10$), the component of the ADTM caused by the light-quenched population is minor, relative to the unquenched $\cos^2\theta$ distribution, and the polarization is 0.282. To avoid confusion, we note that these two populations, before and after the quenching pulse, do not exist at the same time, but both populations contribute to the steady-state polarization.

Phenomenological theory for time-resolved studies of two-beam light quenching

We now consider the effects the time-delayed quenching pulses on the time-resolved intensity and anisotropy decays. In particular, we consider how the step-changes in intensity and anisotropy will effect frequency-domain data (Gratton and Limkeman, 1983; Laczko et al., 1990). The effects of a time-delayed quenching pulse on the intensity and anisotropy decays can be modeled in simple phenomenological terms. Assume that the intensity and anisotropy decay with a lifetime τ and a correlation time Θ, respectively, and that the anisotropy in the absence of rotational diffusion is given by r_0. We assume that the time-delayed pulse, arriving at time $t = t_d$, results in an instantaneous fractional decrease in intensity and anisotropy. It is apparent from the preceding sections that the extent of light quenching will depend on the orientation of the excited-state population and, hence, the ratio of τ to Θ. We have not included this effect in our model, except to recognize that the quenching beam will cause a step-change in the intensity or anisotropy decay.

The fractional decrease in time-dependent intensity is described by

$$q = \frac{I_b - I_a}{I_b}, \tag{60}$$

where I_b and I_a are the intensities immediately before and after the quenching pulse. Because the intensities I_b and I_a are proportional to the respective numbers n_b and n_a of the excited molecules, the parameter q has exactly the same meaning as that introduced by Eq. 43. The fluorescence intensity decay then has the form

$$I(t) = \begin{cases} I_0 e^{-t/\tau} & \text{for} \quad 0 \le t \le t_d, \\ I_0(1-q)e^{-t/\tau} & \text{for} \quad t > t_d. \end{cases} \tag{61}$$

The phase angle (φ_ω) and modulation (m_ω) at each modulation frequency (ω, rad/s) can be computed as (Lakowicz et al., 1984; Gratton et al., 1984)

$$\tan \varphi_\omega = N_\omega / D_\omega \tag{62}$$

$$m_\omega = \frac{1}{J}\sqrt{N_\omega^2 + D_\omega^2}, \tag{63}$$

where the quantities N_ω and D_ω are the sine and cosine Fourier transforms of the fluorescence intensity decay, and J is

the steady-state intensity of the fluorescence. For the decay law described by Eq. 61

$$N_\omega = I_0 \frac{\tau}{1+\omega^2\tau^2} \times \{\omega\tau - [\sin(\omega t_d) + \omega\tau\cos(\omega t_d)]qe^{-t_d/\tau}\}, \quad (64)$$

$$D_\omega = I_0 \frac{\tau}{1+\omega^2\tau^2} \times \{1 - [\cos(\omega t_d) - \omega\tau\sin(\omega t_d)]qe^{-t_d/\tau}\}, \quad (65)$$

$$J = I_0\tau(1 - qe^{-t_d/\tau}). \quad (66)$$

These expressions (Eqs. 64–66) can be used to predict the frequency response for any assumed values of q, t_d or τ.

The frequency-domain anisotropy data can be simulated in a similar manner. The instantaneous change in anisotropy at time $t = t_d$ is described by

$$\Delta r = r_a - r_b = r_a - r_0 e^{-t_d/\Theta}, \quad (67)$$

where r_b and r_a are the anisotropies immediately before and after the quenching pulse. The fluorescence anisotropy decay then has the form

$$r(t) = \begin{cases} r_0 e^{-t/\Theta} & \text{for } 0 \le t \le t_d, \\ (r_0 + \Delta r e^{t_d/\Theta})\, e^{-t/\Theta} & \text{for } t > t_d. \end{cases} \quad (68)$$

In this section, we restrict ourselves to cases where the ADTM displays the z axis symmetry. Then the time-resolved anisotropy is described by Eq. 3 and the intensity decay of the parallel and perpendicular components are given by

$$I_\parallel(t) = \begin{cases} \tfrac{1}{3}I_0\, e^{-t/\tau}[1 + 2\, r_0\, e^{-t/\Theta}] & \text{for } 0 < t \le t_d, \\ \tfrac{1}{3}(1-q)I_0\, e^{-t/\tau}[1 + 2(r_0 e^{-t_d/\Theta} + \Delta r)e^{-(t-t_d)/\Theta}] & \text{for } t > t_d, \end{cases} \quad (69)$$

$$I_\perp(t) = \begin{cases} \tfrac{1}{3}I_0\, e^{-t/\tau}[1 - r_0\, e^{-t/\Theta}] & \text{for } 0 < t \le t_d, \\ \tfrac{1}{3}(1-q)I_0\, e^{-t/\tau}[1 - (r_0 e^{-t_d/\Theta} + \Delta r)\, e^{-(t-t_d)/\Theta}] & \text{for } t > t_d, \end{cases} \quad (70)$$

The frequency-dependent phase difference Δ_ω between the perpendicular and parallel components of the modulated emission, and the ratio Λ_ω of the AC amplitudes of the components, can be calculated from Eqs. 69 and 70 and the well known expressions for differential polarization phase and modulation data (Weber, 1977; Lakowicz et al., 1993, 1987).

$$\Delta_\omega = \arctan\left(\frac{D_\parallel N_\perp - N_\parallel D_\perp}{N_\parallel N_\perp + D_\parallel D_\perp}\right), \quad (71)$$

$$\Lambda_\omega = \frac{\sqrt{N_\parallel^2 + D_\parallel^2}}{\sqrt{N_\perp^2 + D_\perp^2}}, \quad (72)$$

where the quantities $N_\parallel$, $N_\perp$, $D_\parallel$, and $D_\perp$ are defined as respective sine or cosine Fourier transforms of the polarized components of the fluorescence decay. For the intensity decays given by Eqs. 69 and 70, one obtains

$$N_\parallel = \tfrac{1}{3}I_0(n_1 + 2n_2), \quad (73)$$

$$D_\parallel = \tfrac{1}{3}I_0(d_1 + 2d_2), \quad (74)$$

$$N_\perp = \tfrac{1}{3}I_0(n_1 - n_2), \quad (75)$$

$$D_\perp = \tfrac{1}{3}I_0(d_1 - d_2), \quad (76)$$

where the quantities n_i and d_i are expressed as

$$n_1 = \frac{\tau}{1+\omega^2\tau^2}\{\omega\tau - [\sin(\omega t_d) + \omega\tau\cos(\omega t_d)]qe^{-t_d/\tau}\}, \quad (77)$$

$$n_2 = \frac{H}{1+\omega^2H^2}\{r_0\omega H - [\sin(\omega t_d) + \omega H\cos(\omega t_d)]Re^{-t_d/H}\}, \quad (78)$$

$$d_1 = \frac{\tau}{1+\omega^2\tau^2}\{1 - [\cos(\omega t_d) - \omega\tau\sin(\omega t_d)]qe^{-t_d/\tau}\}, \quad (79)$$

$$d_2 = \frac{H}{1+\omega^2H^2}\{r_0 - [\cos(\omega t_d) - \omega H\sin(\omega t_d)]Re^{-t_d/H}\}, \quad (80)$$

with

$$\frac{1}{H} = \frac{1}{\tau} + \frac{1}{\Theta}, \quad (81)$$

$$R = r_0 - (1-q)(r_0 + \Delta r e^{t_d/\Theta}) \quad (82)$$

Effect of two-beam light quenching on the intensity decays

Measurements of time-resolved fluorescence are often performed using frequency-domain methods. Hence, we consider the effects of a step-decrease in the intensity decay on the frequency-domain data. Simulated FD data for a 60% decrease in the excited-state population are shown in Fig. 18. The step-decrease in intensity results in oscillations in the frequency response. These oscillations are particularly evident in the phase data, but are also visible in the modulation data. The frequency of the oscillations is related to the time-delay between the excitation and quenching pulses. The results shown in Fig. 18 suggest that it will be readily possible to detect even small amounts of light quenching from the frequency-domain measurements. In fact, such oscillations have already been observed for a two-beam light quenching experiment (Gryczyński et al., 1994a, b). Depending upon the relative magnitude of σ_a and σ_{lq}, or σ_a for two-photon excitation, it is possible that the second pulse will result in more excitation than quenching. In this case, the oscillations in phase angle will start in the opposite manner, with the phase (*dotted line*) initially becoming larger than the frequency response in the absence of light quenching ($q = 0$, *dashed line*). If the excitation and quenching pulses are time-coincident, then there is no change in shape of the intensity

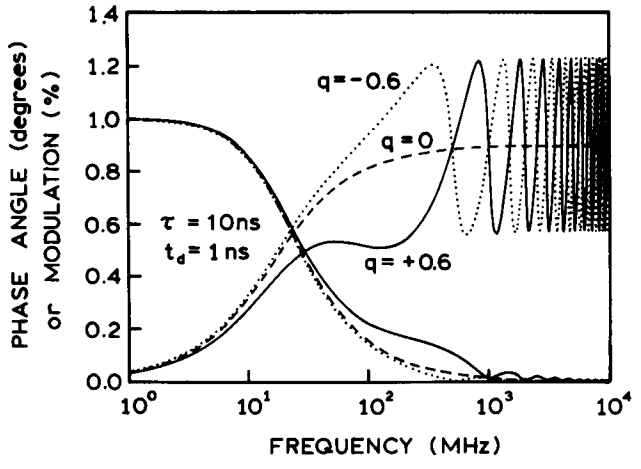

FIGURE 18 Simulated effect of light quenching on the frequency response of a fluorophore with a 10 ns decay time (——). The delay time is 1 ns. The dashed line shows the unquenched data. The dotted line ($q = -0.6$) indicates excess excitation over quenching by the delayed pulse.

decay. Hence, the decay time and frequency response remain unchanged irrespective of the extent of light quenching.

Effect of two-beam light quenching on the frequency-domain anisotropy decays

Two-beam light quenching can result in a profound alteration of the frequency-domain anisotropy decay. Simulated results for 60% light quenching, and $\Delta r = -0.26$, with $\tau = 10$ ns and $\Theta = 1$ ns, are shown in Fig. 19. The time-domain intensity and anisotropy decays for these assumed values are shown as an insert in Fig. 19. The anisotropy is 0.15 upon arrival of the quenching pulse at $t_d = 1$ ns. The change in anisotropy of $\Delta r = -0.26$ was used because it is near the expected value for the assumed parameter values (see below). The step-change in the anisotropy results in oscillations in the differential polarized phase angles and the modulated anisotropy. The depth of the oscillations is sensitive to the extent of quenching (not shown), and the rate of the oscillation depends on the time-delay. Examination of Fig. 19 reveals that the modulated anisotropy can exceed the usual upper limit of 0.4 because of the step-change in anisotropy and its effect on the frequency response.

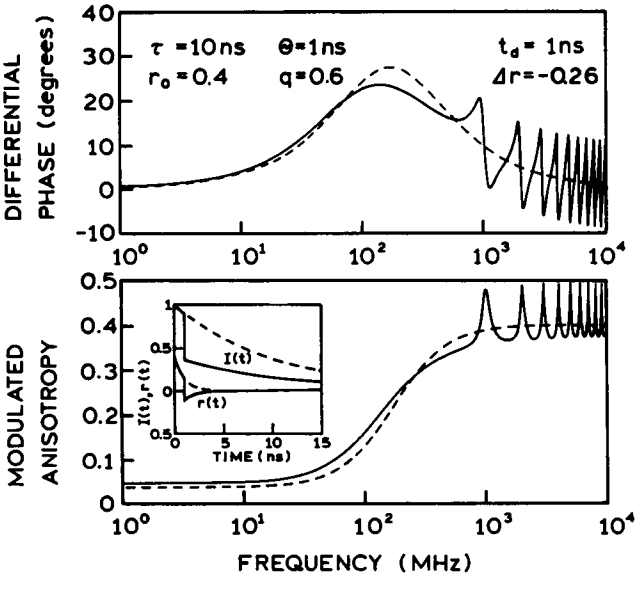

FIGURE 19 Effect of parallel light quenching on the frequency-domain anisotropy data. The quenching pulse arrives at time $t_d = 1$ ns and decreases the total intensity by 60%. The emission anisotropy is equal to 0.15 immediately before the light quenching and is assumed to drop to −0.11 immediately after the quenching pulse. The corresponding effect of the light quenching on the time-domain data is shown in the inset. The dashed lines show the unquenched data.

The oscillations shown in Fig. 19 are unique property of a two-beam experiment. If the time delay is decreased to 0.001 ns, then the frequency-domain anisotropy data become almost identical to that observed for a fluorophore with a lifetime (τ) of 10 ns and correlation time (Θ) of 1 ns, but with a decreased time-zero anisotropy (Fig. 20, *left panels*). If the time-delay is increased to 10 ns, then the frequency of the oscillations increases (Fig. 20, *right panels*). The amplitude of the oscillation is decreased, relative to Fig. 19 with $t_d = 1.0$ ns, because of the longer delay time and less quenching of the total emission. These simulations suggest that the frequency-domain anisotropy decay measurements will provide a sensitive method to study the effects of light quenching.

Relationship of the extent of quenching to the change in anisotropy

In practice, the parameters q and Δr are related. We now only consider the relationship between q and Δr for parallel quenching in two limiting cases, when the delay time t_d is very large or very small compared with rotational correlation time Θ. Assume at first that $t_d/\Theta \ll 1$. In this case, rotational diffusion does occur before arrival of the quenching pulse, and the time evolution of the ADTM is described by the equations derived in previous sections. The anisotropy r_a immediately after (a) the quenching pulse can be calculated as

$$r_a = \frac{I_{a\parallel} - I_{a\perp}}{I_{a\parallel} + 2I_{a\perp}} \tag{83}$$

The intensities $I_{a\parallel}$ and $I_{a\perp}$ can be found from Eqs. 1 and 2 by setting $t = t_d$ and integrating over φ

$$I_{a\parallel} = c_1 2\pi \int_0^{\pi/2} n_a(\theta, t_d)\cos^2\theta \sin\theta \, d\theta, \tag{84}$$

$$I_{a\perp} = c_1 \pi \int_0^{\pi/2} n_a(\theta, t_d)\,(1 - \cos^2\theta)\sin\theta \, d\theta, \tag{85}$$

where the function $n_a(\theta, t_d)$ describes the ADTM immediately after the quenching pulse and is given by the second line of Eq. 44. The parameter Δr can be then calculated from Eq. 67, with $r_0 = 0.4$ and $t_d/\Theta = 0$. Note that in this case, Δr does not depend on the delay time t_d, but is, of course, dependent

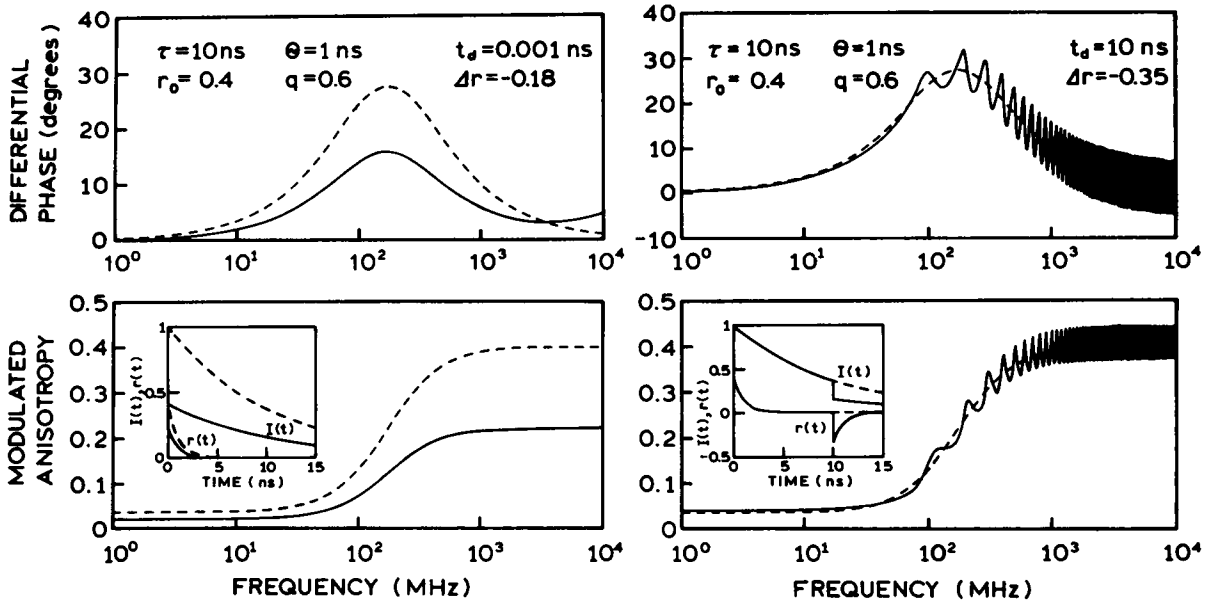

FIGURE 20 Effect of parallel light quenching on the frequency-domain anisotropy data. The two panels show simulations as the time-delay of light quenching pulse is increased from t_q = 0.001 ns (*left*) to 10 ns (*right*). The decay time and correlation times are assumed to be 10 and 1 ns, respectively. The dashed lines show the unquenched frequency-domain anisotropy data.

on the parameter S_{p2}. The value of the parameter q, which is associated with a calculated value of the anisotropy decrease Δr, may be evaluated from Eq. 43 using the same value of S_{p2}.

In the second limiting case, when $t_d/\Theta \gg 1$, the same formalism may be applied. The only difference is that now the function $n_0(\theta)$ in the second line of Eq. 44 has to be replaced by a constant, to indicate that the shape of the ADTM immediately before the light quenching is spherical. This correlation between q and Δr was taken into account in the simulations on the frequency-domain anisotropy data shown in Figs. 19 and 20. We use a value of $\Delta r = -0.26$, which is the average of that expected for $t_d \gg \Theta$ and $t_d \ll \Theta$ for the assumed value of $q = 0.6$.

DISCUSSION

The previous section described the types of oriented fluorophore populations that can be achieved with light quenching and how the intensity and anisotropy decays are altered by a time-delayed quenching pulse. Considerably more detail is required to provide a complete description that includes the effects of rotational diffusion, spectral relaxation, ground-state depletion, non-colinear transition moments, and the effects of pulse width, to name a few. Based on our recent experimental studies with light quenching of several fluorophores (Lakowicz et al., 1994; Gryczyński et al., 1993, 1994), we feel the results described above are experimentally achievable. Using one-beam experiments (Gryczyński et al., 1993, 1994), we have already demonstrated that significant amounts of light quenching can be observed using commercially available ps lasers and that the light quenching occurred without significant photochemical damage. Additionally, the light quenching data demonstrated that the extent of quenching is proportional to the amplitude of the emission spectrum at the quenching wavelength and that light quenching is accompanied by a decrease in the time-zero anisotropy. It is important to note that light quenching is not the same as polarized photobleaching, in which case part of the fluorophore population is destroyed by a bleaching pulse at the absorption wavelength. In the case of light quenching, the fluorophore will typically be illuminated at nonabsorbed wavelengths, and the effects we describe do not require that any fluorophores be destroyed.

Light quenching is accomplished using intense illumination at wavelengths longer than the absorption spectrum. It is thus natural to question whether the extent of two-photon excitation will be larger than the extent of light quenching. We have found that this is not necessarily the case, and light quenching can be the dominant effect. For instance, we were able to observe light quenching of Rhodamine B (Lakowicz et al., 1994) and the laser dye DCM (Gryczynski et al., 1994) using one-photon excitation on the long wavelength side of the emission spectra. We note that TPE is best accomplished with fs sources, because the extent of two-photon absorption is proportional to the square of the peak power. In contrast, light quenching is a linear process and is proportional to the total number of photons passing near the excited fluorophore. Hence, light quenching can be accomplishing with the 5–10 ps pulses from mode-locked ion or Nd:YAG lasers with minimal two-photon absorption.

And finally we note that technological advances in commercially available lasers is resulting in the increasing possibility and practicality of the two-beam experiments described above. For instance, it is now possible to buy synchronized mode-locked Ti:Sapphire lasers, where the

time delays between the pulses are readily adjustable. One laser can be a ps or fs laser appropriate for excitation, and the second can be ps or wider pulses to maximize energy or minimize TPE. Ti:Sapphire laser sources have been used in regenerative amplifiers to obtain intense Q-switched pulses at kHz rates (Seaton, 1993). Additionally, it is possible to obtain Q-switch laser sources with the output centered near 355 nm, the emission maxima of proteins.

In conclusion, multi-pulse time-resolved light quenching offers new opportunities for the use of time-resolved fluorescence in the study of chemical and biochemical systems.

This work was supported by grants from the National Science Foundation (DIR-8710401 and BIR-9319032) and National Institutes of Health (BR-08119). J. R. Lakowicz expresses appreciation to the Medical Biotechnology Center at the University of Maryland at Baltimore.

REFERENCES

Ansari, A., and A. Szabo. 1993. Theory of photoselection by intense light pulses: influence of reorientational dynamics and chemical kinetics on absorbance measurements. *Biophys. J.* 64:838–851.

Baeyens, W. R. G., D. De Keukeleire, and K. Korkidis, editors. 1991. Luminescence Techniques in Chemical and Biochemical Analysis. Marcel Dekker, Inc., New York 654 pp.

Demas, J. N. 1983. Excited State Lifetime Measurements. Academic Press, London. 273 pp.

Demchenko, A. P. 1986. Ultraviolet Spectroscopy of Proteins Springer Verlag, Berlin. 312 pp.

Denk, W., J. H. Strickler, and W. W. Webb. 1990. Two-photon laser scanning fluorescence microscopy. *Science.* 248:73–76.

Dewey, T. G., editor. 1991. Biophysical and Biochemical Aspects of Fluorescence Spectroscopy. Plenum Press, New York. 294 pp.

Einstein, A. 1917. On the quantum theory of radiation. *Phys. Z.* 18:121–128. (This paper has been reprinted in Laser Theory by F. S. Barnes, IEEE Press, New York, 1972).

Fleming, G. R. 1986. Chemical Applications of Ultrafast Spectroscopy. Oxford University Press, New York. 262 pp.

Gratton, E., J. R. Lakowicz, B. Maliwal, H. Cherek, G. Laczko, and M. Limkeman. 1984. Resolution of mixtures of fluorophores using variable-frequency phase and modulation data. *Biophys. J.* 46:479–486.

Gratton, E., and M. Limkeman. 1983. A continuously variable frequency cross-correlation phase fluorometer with picosecond resolution. *Biophys. J.* 44:315–324.

Gryczyński, I., V. Bogdanov, and J. R. Lakowicz. 1993. Light quenching of tetraphenylbutadiene fluorescence observed during two-photon excitation. *J. Fluorescence.* 3:85–92.

Gryczyński, I., V. Bogdanov, and J. R. Lakowicz. 1994. Light quenching and depolarization of fluorescence observed with a high repetition rate picosecond dye laser. *Biophys. Chem.* 49:223–232.

Gryczyński, I., J. Kuśba, V. Bogdanov, and J. R. Lakowicz. 1994a. Control of excited state population by light quenching of fluorescence. *Proc. SPIE.* 2137:742–760.

Gryczyński, I., J. Kuśba, and J. R. Lakowicz. 1994b. Light quenching of fluorescence using time-delayed laser pulses as observed by frequency-domain fluorometry. *J. Phys. Chem.* In press.

Jabloński, A. 1967. Fundamental polarization of photoluminescence of solution (in Polish). *Postepy Fiz.* 18:663–672.

Jameson, D. M., and G. D. Reinhart, editors. 1989. Fluorescent Biomolecules: Methodologies and Applications. Plenum Press, New York. 461 pp.

Klein, U. K. A. 1984. Picosecond fluorescence decay studied by phase fluorometry and its application to the measurement of rotational diffusion in lipids. *Arab. J. Sci. Eng.* 17:261–286.

Koppel, D. E., P. Primakoff, and D. G. Myles. 1986. Fluorescence photobleaching analysis of cell surface regionalization. *In* Applications of Fluorescence in the Biomedical Sciences. D. L. Taylor, A. S. Waggoner, R. F. Murphy, F. Lanni, and R. R. Birge, editors. A. R. Liss, Inc., New York. 477–497.

Laczko, G., J. R. Lakowicz, I. Gryczyński, Z. Gryczyński, and H. Malak. 1990. A 10 GHz frequency-domain fluorometer. *Rev. Sci. Instrum.* 61: 2331–2337.

Lakowicz, J. R., editor. 1992. Time resolved laser spectroscopy in biochemistry III. January 20–22, Los Angeles, CA. *Proc. SPIE.* 1640:807.

Lakowicz, J. R., H. Cherek, I. Gryczynski, N. Joshi, and M. L. Johnson. 1987. Enhanced resolution of fluorescence anisotropy decay by simultaneous analysis of progressively quenched samples: applications to anisotropic rotations and protein dynamics. *Biophys. J.* 51:755–768.

Lakowicz, J. R., H. Cherek, J. Kuśba, I. Gryczyński, and M. L. Johnson. 1993. Review of fluorescence anisotropy decay analysis by frequency-domain fluorescence spectroscopy. *J. Fluorescence.* 3:103–116.

Lakowicz, J. R., E. Gratton, G. Laczko, H. Cherek, and M. Limkeman. 1984. Analysis of fluorescence decay kinetics from variable-frequency phase shift and modulation data. *Biophys. J.* 46:463–477.

Lakowicz, J. R., and I. Gryczyński. 1991. Frequency-domain fluorescence spectroscopy. *In* Topics in Fluorescence Spectroscopy: Techniques, Vol. 1. J. R. Lakowicz, editor. Plenum Press, New York. 293–235.

Lakowicz, J. R., and I. Gryczyński. 1992. Fluorescence intensity and anisotropy decay of the 4′,6-diamidino-2-phenylindole-DNA complex resulting from one-photon and two-photon excitation. *J. Fluorescence.* 2: 117–122.

Lakowicz, J. R., I. Gryczyński, V. Bogdanov, and J. Kuśba. 1994. Light quenching and fluorescence depolarization of rhodamine B. *J. Phys. Chem.* 98:334–342.

Lakowicz, J. R., I. Gryczyński, E. Danielsen, and J. K. Frisoli. 1992a. Unexpected anisotropy spectra of indole and *N*-acetyl-L-tryptophanamide observed for two-photon excitation of fluorescence. *Chem. Phys. Lett.* 194:282–287.

Lakowicz, J. R., I. Gryczyński, Z. Gryczyński, D. Danielsen, and M. J. Wirth. 1992b. Time-resolved fluorescence intensity and anisotropy decays of 2,5 diphenyloxazole by two-photon excitation and frequency-domain fluorometry. *J. Phys. Chem.* 96:3000–3006.

Lakowicz, J. R., I. Gryczyński, J. Kuśba, and E. Danielson. 1992c. Two photon-induced fluorescence intensity and anisotropy decays of diphenylhexatriene in solvents and lipid bilayers. *J. Fluorescence.* 2: 247–258.

Mazurenko, Y. T. 1973. Polarization of luminescence of complex molecules under quenching by light. *Opt. Spectrosc.* 35:137–139.

Michl, J., and E. W. Thulstrup. 1986. Spectroscopy with Polarized Light, VCH Publishing, New York. 573 pp.

O'Connor, D. V., and D. Phillips. 1984. Time-correlated Single Photon Counting. Academic Press, London. 288 pp.

Piston, D. W., D. R. Sandison, and W. W. Webb. 1992. Time-resolved fluorescence imaging and background rejection by two-photon excitation in laser scanning microscopy. *Proc SPIE.* 1640:379–389.

Seaton, C. T. 1993. Simplified fast-pulsed lasers broaden research vistas. *Photonics Spec.* 150–154.

Szmacinski, H. S., I. Gryczyński, and J. R. Lakowicz. 1993. Calcium-dependent fluorescence lifetimes of indo-1 for one- and two-photon excitation of fluorescence. *Photochem. Photobiol.* 58:341–345.

Weber, G. 1977. Theory of differential phase fluorometry: detection of anisotropic molecular rotations. *J. Chem. Phys.* 66:4081–4091.